The Meteoritical Society

Meteoritics & Planetary Science 45, Nr 9, 1502–1512 (2010)
doi: 10.1111/j.1945-5100.2010.01125.x

Basaltic micrometeorites from the Novaya Zemlya glacier

Dmitry D. BADJUKOV[1*], Franz BRANDSTÄTTER[2], Jouko RAITALA[3], and Gero KURAT[2†]

[1]V. I. Vernadsky Institute of Geochemistry and Analytical Chemistry RAS, 19, Kosygin str., 119991, Moscow, Russia
[2]Naturhistorisches Museum, Burgring 7, Wien A-1010, Austria
[3]Astronomy, Department of Physical Sciences, P.O. box 3000, FIN-90014 University of Oulu, Oulu, Finland
[†]Deceased.
[*]Corresponding author. E-mail: badyukov@geokhi.ru

(Received 12 November 2009; revision accepted 13 August 2010)

Abstract–A large number of micrometeorites (MMs) was recovered from glacier deposits located at the north-eastern passive margin of the Novaya Zemlya glacier sheet. Melted, scoriaceous, and unmelted micrometeorites (UMMs) are present. Unmelted micrometeorites are dominated mostly by chondritic matter, but also a few achondritic MMs are present. Here we report the discovery of four UMMs that, according to their texture, mineralogy, and chemistry, are identified as basaltic breccias. Mineral chemistry and Fe/Mn ratios of two basaltic micrometeorites indicate a possible relationship with eucrites and/or mesosiderites, whereas two others seem to have parents, which appear not to be present in our meteorite collections. The basaltic breccia UMMs constitute 0.5% of the total population of the Novaya Zemlya MM suite. This content should be lowered to 0.25% because the Novaya Zemlya MM collection appears to be biased with carbonaceous UMMs being underrepresented.

INTRODUCTION

The flux of extraterrestrial material to the Earth is around 30,000 t/a (Love and Brownlee 1993; Peucker-Ehrenbrink and Ravizza 2000). The accreted material consists mostly of interplanetary dust particles that interact with the atmosphere and reach the Earth's surface as cosmic spheres (CSs) or micrometeorites (MMs). The MM accretion rate has been estimated to lie in a range from 2,700 to 14,000 t/a (Taylor et al. 1998; Yada et al. 2004) and it overwhelms the meteorite flux, which is approximately 50 t/a (Halliday et al. 1989). The dust accretion rates of the Earth as estimated from MMs in Antarctic ice are fairly compatible with those measured outside the Earth's atmosphere, because uncertainties in the estimations are as high as 50% if evaporation and disruption of interplanetary dust particles during their atmospheric entry are taken into the account.

Antarctic and Arctic glacier surfaces are good collectors of terrestrial and extraterrestrial dust (Maurette 2006). During the last 35 yr, a huge number of MMs were collected from glaciers of Antarctica by melting of ice or snow (Maurette et al. 1991; Taylor et al. 2000; Yada et al. 2004; Duprat et al. 2007). Other MM-rich deposits are glacier lake sediments (Maurette et al. 1986, 1987) and deep-sea sediments (Blanchard et al. 1980; Taylor and Brownlee 1991).

It has been established that MMs are related mostly to carbonaceous chondrites (Kurat et al. 1994; Engrand and Maurette 1998). The abundance of ordinary chondrite-related MMs in the MM stream is not well defined, they could comprise only about 1% of all MMs (Walter et al. 1995) or around 20–30% (Genge 2008; Suavet et al. 2010). In any case, the abundances differ from the relative abundances of meteorite classes. Statistics of meteorite falls show that the meteorite flux consists of ordinary chondrites (77.1%), achondrites (8.1%), irons (5%), and carbonaceous chondrites (3.8%) (Grady 2000). A minor mineralogical difference between MMs and chondritic meteorites is shown by the very rare occurrence of chondrules and their fragments in the collected MMs (Walter et al. 1995; Kurat et al. 1996; Genge et al. 2005). This

© The Meteoritical Society, 2010.

compositional discrepancy between MM and meteorite populations can be connected with a number of factors including

1. Different sources of MMs and meteorites,
2. Different comminution behavior of carbonaceous and ordinary chondrites in asteroidal collisions, or
3. Different delivery mechanism for various sizes of meteoroids from the asteroidal belt to the Earth.

It has been proposed that MMs might originate from comets (Maurette et al. 1996; Maurette 2006). On the other hand, asteroids have been considered as the main source of MMs (Love and Brownlee 1991; Brownlee et al. 1997).

If MMs are originally from the asteroid belt, they should comprise also achondritic rocks—as well as irons and stony iron components. However, despite a vast number of studied MMs, only one unmelted achondritic MM was found so far (Gounelle et al. 2009). Among numerous melted MMs, only a few spherules have compositions and Fe/Mn ratios close to those of eucrites, and some of them contain relic inclusions of silica and Ca-rich feldspar (Taylor et al. 2007a). Here we report on the identification of unmelted basaltic MMs from the glacier of Novaya Zemlya. Mineralogically and compositionally they are very close to basaltic eucrites, although they may differ from basaltic eucrites in details.

COLLECTION SITE, SAMPLES AND METHODS

The glacier sheet of the Northern Island of the Novaya Zemlya archipelago covers approximately 55% of the island's territory. The island is 430 km long, 40 to 45 km wide, and 0.9 km high. The maximal age of the glacier ice is estimated to be less than 1 kyr (Koryakin 1990), and this is also the maximum age of the oldest solid fraction present in the ice. The northeastern part of the sheet is characterized by passive margins where glacier ice contains solid components including accumulated MMs. The glacier seems to have negative annual mass balances (Badjukov and Raitala 2003). This makes the marginal glacier areas with solid component concentrations to be very suitable places to find fine-grained samples that may contain MMs.

The edges of the glacier margins have a smooth surface with an outward slope of a few degrees. The border zone between glacier and the country rock has an edge moraine that consists of a mixture of unsorted bedrock debris and ice. The local folded Triassic sedimentary bedrocks consist of black and gray siltstone, shale, and fine-grained sandstone. Patches of clayish appearing matter are located on the ice surface close to the moraine-glacier border, which consists of accumulated beads of possibly cryoconite. During the 2006 field season (Fig. 1) we sampled the moraine and the clayish appearing matter.

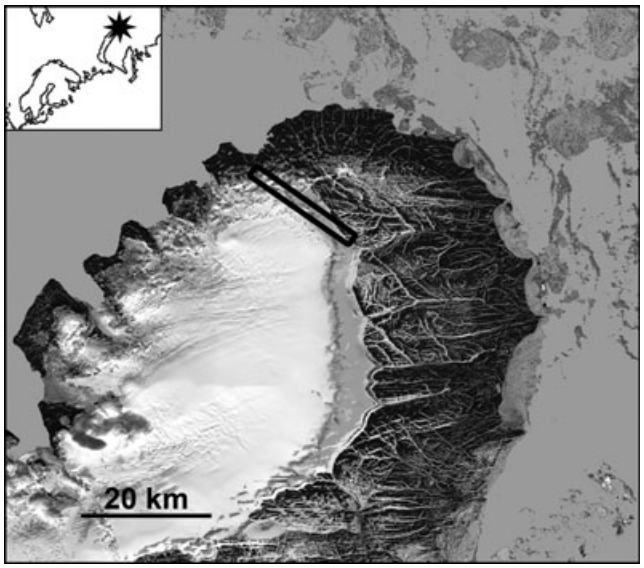

Fig. 1. The Landsat 7 image shows the northern part of North Island of the Novaya Zemlya archipelago. The location of the image is shown by an asterisk in the insertion (left upper corner). The area of the fieldwork is marked by a rectangle on the image.

In the laboratory, the samples were extracted from the plastic bags and wet-sieved using a set of plastic sieves. The sample preparation was performed in a room that was never before used for work on meteoritic matter. After sieving the 50–100, 100–250, and 250–500 μm fractions, we electromagnetically removed quartz, alkali feldspars, mica, organic material, and other particles derived from local sediments. The electromagnetic parts of the fractions were examined under an optical microscope and all particles that appeared to be somehow distinct from local rocks were picked out. The particles were embedded in epoxy, polished, and studied at the Oulu University, Finland, and the Naturhistorisches Museum in Vienna with scanning electron microscopes JEOL JSM-6400 equipped with energy dispersive X-ray (EDX) analysis systems. Micrometeorite identification used criteria like a chondritic EDX spectrum, the presence of magnetite rims, mineral composition, and specific textures. Compositions of minerals and matrices of MMs were measured using the JEOL JXA-8200 electron microprobe at the Oulu University operated at 15 kV with a beam current of 15 nA. Bulk chemistry was determined with a defocused 10 or 20 μm beam depending on the particle structure. The microprobe was calibrated on standard oxides and silicates and the data were reduced using the ZAF JEOL program. Detection limits are approximately 0.02 wt% for all elements.

An attempt was made to establish shock effects in minerals in particles of interest, especially by looking for plagioclase and silica in amorphous state. Epoxy tablets with the particles were thinned to approximately 1 mm thickness and studied in transmitted light using a Leica optical microscope. Unfortunately, because some of the studied grains were superimposed on birefrigent pyroxene and opaque iron oxide shells were present, decisive observations were not possible in some cases. Micro-Raman studies were performed with the same goal. The micro-Raman measurements were carried out at the Physical Faculty of the Moscow State University, Russia using a LabRAM HR Visible spectrometer with a 15 mW, 632.8 nm He/Ne-laser excitation system and a CCD detector. The spectra were collected in the range of 100–1200 cm^{-1}. The spectral resolution was 3 cm^{-1} using a grating with 1800 grooves per mm. The measurements were performed using a 50× objective on the Raman microscope with approximately 30 s acquisition time and a spot size of 3 μm. The spectra were corrected for luminescence backgrounds, and the experimental data were treated by linearly interpolating of backgrounds over the whole frequency range and subtracting of obtained background values from experimental spectra.

RESULTS

No extraterrestrial particles were found in the moraine samples of total weight of 25 kg, whereas the clayish matter from the surface patches contains numerous MMs. The maximum MM concentration was approximately 150 particles per gram in the fractions studied.

Our collection contains cosmic spherules (CS, melted MMs), scoriaceous MMs, and unmelted MMs (UMMs). Most UMMs are completely or partially enveloped by iron oxide rims and mainly consist both of phyllosilicates or their thermal dehydration products and of pyroxene and/or olivine. The particles are classified as different fine-grained and coarse-grained MM types (Genge et al. 2008), respectively. It has been suggested (Kurat et al. 1994; Engrand and Maurette 1998; Genge 2008) that the MMs are relatives of chondrite constituents (e.g., their matrices, aggregates, and chondrules). However, there is a small number of particles that drastically differs from the fine- and coarse-grained chondrite MMs in textures, mineralogy, and chemistry.

This group is composed of four particles (Fig. 2) that are classified as basaltic melt breccias. They have irregular shapes and are transected by cracks; two of them contain vesicles. Particles NZ6-2-5,15 and NZ6-2-4,5 have a discontinuous magnetite rim. The constituent phases are low- and high-Ca pyroxenes, plagioclase, silica, ilmenite, chromite, and glass. Textures of the particles NZ6-1-1,44, NZ6-2-4,33, and NZ6-2-4,5 are characterized by angular mineral fragments of different sizes embedded in various glassy matrices. Matrix glass of particle NZ6-2-4,33 is rich in tiny iron oxide grains; the matrix of particle NZ6-2-4,5 contains regions consisting of glass with inclusions of elongated anhedral pyroxene(?) grains; pyroxene and plagioclase phase fragments in particle NZ6-2-5,15 are cemented by pyroxene-rich glass dusted with silica and oxide(s) grains. Pyroxene fragments in particle NZ6-2-4,33 show thin reaction borders toward the glassy matrix and one pyroxene clast in particle NZ6-2-4,5 seems to be partially melted.

Compositions and habits of pyroxenes in individual particles differ from each other (Table 1). Low-Ca pyroxene in particle NZ6-1-1,44 has exsolutions of augitic pyroxene lamellae in pigeonite, whereas low-Ca pyroxenes of other particles are homogeneous. The low-Ca pyroxenes in the particles range in compositions from Fs_{13} to Fs_{60} and from Wo_1 to $Wo_{7.}$ The pyroxenes of particle NZ6-2-4,5 have the lowest iron content ($Fs_{13–17}$) and a high Ca content ($Wo_{5–7}$). Pyroxenes of others are more iron rich—$Fs_{21–35}Wo_{1–3}$, $Fs_{49–55}Wo_{2–6}$, and $Fs_{57–60}$ $Wo_{5–7}$ in particles NZ6-1-1,44, NZ6-2-4,33, and NZ6-2-5,15, respectively. The TiO_2, Al_2O_3, and Cr_2O_3 contents are usually below 1 wt% and the Fe/Mn ratio ranges from 10 to 35.

The high-Ca pyroxene of particle NZ6-2-5,15 has exsolution lamellae of low-Ca pyroxene. On the other hand, the pyroxenes in particles NZ6-2-5,15 and NZ6-2-4,5 are free of exsolutions but chemically inhomogeneous. The particle NZ6-2-4,33 lacks high-Ca pyroxene.

Compositions of high-Ca pyroxenes are different also among studied particles: Fs contents vary between 35–42, 42–48, and 5–6 mole% and Wo contents range between 19–24, 18–24, and 38–44 mole% in particles NZ6-1-1,44, NZ6-2-5,15, and NZ6-2-4,5, respectively. It has to be noted that certain variations in Ca, Mg, and Fe can be due to the measuring geometry that resulted in a partial signal from an adjacent low- or high-Ca pyroxene lamellae when performing the microprobe analysis. Pyroxene grains in NZ6-2-4,33 have thin rims enriched in Fe. The Fe/Mn atomic ratios of the pyroxenes are 23–25, 32, and 12–15 for particles NZ6-1-1,44, NZ6-2-5,15, and NZ6-2-4,5, respectively. The Na_2O content is around 0.6 wt% in pyroxenes of particle NZ6-2-4,5.

Calcic plagioclase phase compositions range from An_{91} to $An_{89.5}$ in particles NZ6-2-4,33 and NZ6-2-5,15; from An_{85} to An_{77} in particle NZ6-1-1,44, and from An_{75} to An_{65} in particle NZ6-2-4,5 (Table 2).

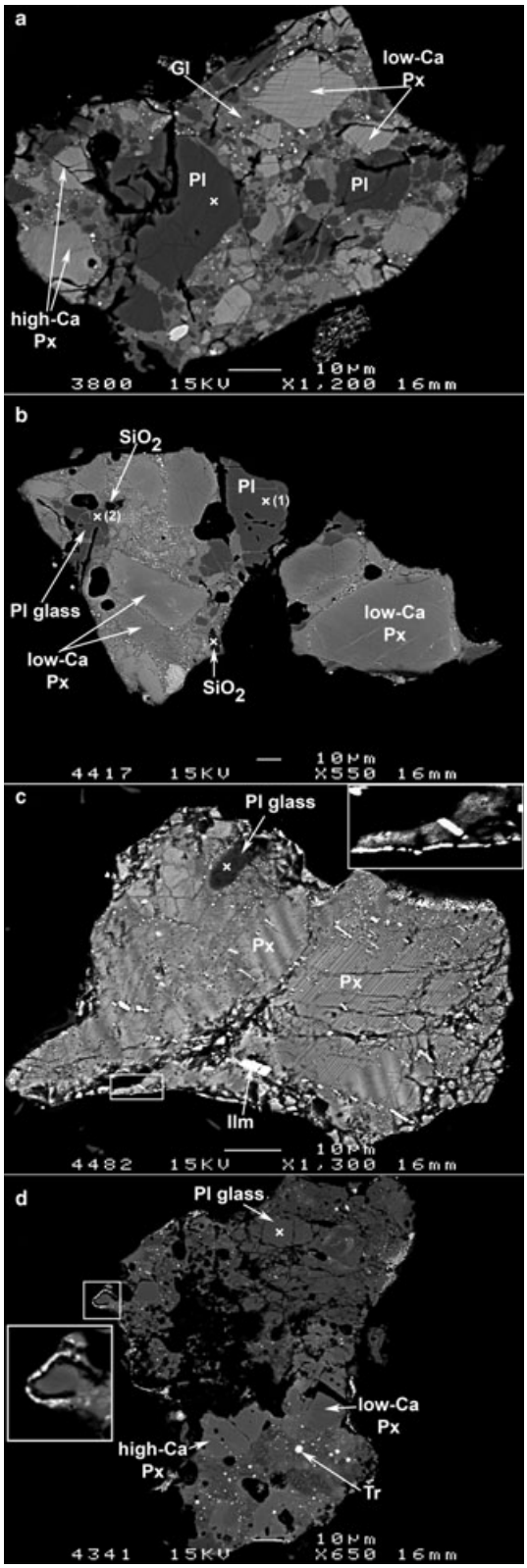

Fig. 2. Backscattered electron images of polished sections of Novaya Zemlya basaltic breccia UMMs. a) Particle NZ6-1-1,44 consists of angular clasts of low-Ca pyroxene (low-Ca Px, gray), high-Ca pyroxene (high-Ca Px, gray), and plagioclase (Pl, dark gray) embedded in glassy matrix (Gl). Light phase is chromite. One low-Ca pyroxene fragment (top center) shows exsolution lamellae. The particle is cut by cracks. The separate small particle (lower right) is a terrestrial contaminant (shale). b) Particle NZ6-2-4,33 consists of low-Ca pyroxene (light gray), plagioclase (Pl, gray), plagioclase glass (Pl glass, gray) and amorphous silica (SiO_2, dark gray) in a glassy matrix. The matrix contains numerous tiny chromite grains (white). Some pyroxene fragments have Fe-rich borders. Due to the irregular shape, the particle section seems to consist of two separate regions. c) Particle NZ6-2-5,15 is dominated by pyroxenes with exsolution lamellae and it contains a rounded inclusion of plagioclase glass (Pl glass, dark gray) on top center. The pyroxene grain contains subparallel platelets of ilmenite (Ilm, white). Dust-like silica inclusions are present in regions of possibly remelted pyroxene (left). The particle is partly enveloped by a thin iron oxide rim. A part of the rim is shown on the insertion. d) Particle NZ6-2-4,5 consists of irregular fragments of pyroxene (Px, gray) and plagioclase glass (Pl glass, dark gray) in porous matrix with troilite (Tr) droplets (white). The matrix consists of glass with pyroxene crystallites. The particle has abundant voids and cracks and it is covered partly by an iron oxide rim. An enlarged detail of the rim is shown on the insertion. X-shaped crosses on the images mark locations of points of micro-Raman analyses (see Fig. 3).

Plagioclase phases in particles NZ6-1-1,44 and NZ6-2-5,15 have slightly elevated amounts of K_2O (up to 0.22 wt%), whereas the K_2O content in plagioclase of the two other particles is less than 0.07 wt%. Plagioclase phases contain some FeO and MgO that vary from 0.15 to 0.65 wt% and from 0 to 0.20 wt%, respectively. Some grains show higher FeO and MgO contents up to 1–2 wt%.

Plagioclase fragments in particle NZ6-1-1,44 are birefringent. The observation is consistent with a Raman spectrum of a plagioclase clast. The spectrum (Fig. 3) displays bands centered at 483, 510, and 565 cm^{-1}, that are attributed as crystalline plagioclase (Matson et al. 1986). All but one plagioclase clasts in particle NZ6-2-4,33 are birefringed and have the Raman spectra (Fig. 3) of crystalline plagioclase whereas one clast seems to be either isotropic or have very weak birefringence. Its Raman spectrum obtained has two broad bands at approximately 500 and 590 cm^{-1} and is similar to spectra of plagioclase glasses of different origin (Matson et al. 1986; Velde et al. 1989). One plagioclase grain in particle NZ6-2-4,5 shows a Raman spectrum (Fig. 3) also to be similar to plagioclase glass spectra. Bands at 680 and 1015 cm^{-1} can be attributed to pyroxene, because they can appear due to small size of the plagioclase grain and capture of adjacent pyroxene by a laser beam. Plagioclase in particle NZ6-2-4,5 seems to be isotropic. Its Raman spectrum does not have any bands excluding a very wide hump of the spectrum over a 300–700 cm^{-1} range (Fig. 3) and is

Table 1. Electron microprobe analyses of pyroxenes from the Novaya Zemlya basaltic UMMs (in wt%).

	NZ6-1-1,44		NZ6-2-4,33		NZ6-2-5,15		NZ6-2-4,5	
UMM	Low-Ca Px	High-Ca Px	Low-Ca Px	High-Ca Px	Low-Ca Px	High-Ca Px	Low-Ca Px	High-Ca Px
SiO_2	50.9	49.4	55.4	53.1	50.2	50.0	55.9	53.5
TiO_2	0.25	0.36	0.05	0.20	0.17	0.19	n.d.	0.06
Al_2O_3	0.36	1.07	0.50	4.82	0.11	0.31	0.70	2.90
Cr_2O_3	0.10	0.44	0.70	0.37	0.08	0.16	0.42	1.26
FeO	31.4	24.5	15.9	16.3	36.5	27.8	9.37	3.86
MnO	1.24	1.01	0.51	0.48	1.15	0.87	0.44	0.23
MgO	12.9	11.7	26.1	20.2	11.8	10.7	29.2	16.1
CaO	2.88	10.5	1.08	4.04	1.18	9.41	3.26	22.3
Na_2O	n.d.	n.d.	0.02	0.08	n.d.	0.03	0.07	0.70
K_2O	n.d.	n.d.	n.d.	n.d.	n.d.	n.d.	n.d.	0.14
Total	99.1	99.0	100.2	99.7	100.7	99.5	99.4	101.2
Fs	54.1	41.6	25.0	28.4	60.5	46.1	14.3	6.3
Wo	6.4	6.4	2.2	9.0	2.5	20	6.4	46.7
Fe/Mn	25	24	30	34	31	31.	21	17

n.d. = not detected.

Table 2. Electron microprobe analyses of plagioclases and plagioclase phases from the Novaya Zemlya basaltic UMMs.

UMM	NZ6-1-1,44	NZ6-2-4,33	NZ6-2-5,15	NZ6-2-4,5
SiO_2	47.0	46.3	46.4	50.1
Al_2O_3	34.5	34.2	33.7	31.6
Cr_2O_3	n.d.	n.d.	n.d.	0.37
FeO	0.30	0.24	0.98	0.28
MnO	0.01	0.01	0.04	0.02
MgO	0.04	0.08	0.12	0.04
CaO	16.9	18.5	18.5	15.2
Na_2O	1.63	0.98	0.90	2.94
K_2O	0.05	0.06	0.12	0.05
Total	100.38	100.28	100.86	100.67
An	84.9	90.9	91.3	74.0
Ab	14.8	8.7	8.0	25.8

n.d. = not detected.

very close to spectra of amorphous plagioclase phases (Fritz et al. 2005).

Silica is present as small irregular grains in particle NZ6-2-4,33 and as tiny pellets in the glassy matrix of particle NZ6-2-5,15. The Raman spectrum of a silica grain contains a broad band centered at about 480 cm^{-1} (Fig. 3) and is typical for SiO_2 in an amorphous state (Gucsik et al. 2003). The matrix glass (Table 3) in particle NZ6-1-1,44 has approximately 50 wt% SiO_2, 13% Al_2O_3, 7% MgO, 16% FeO, 0.6% MnO, 11% CaO, and 0.3% Na_2O. Glassy areas in the particle NZ6-2-4,5 are chemically inhomogeneous and contain 67–73 wt% SiO_2, 22% Al_2O_3, 0.1–0.7% MgO, 0.1–1% FeO, 2% CaO, 1–5% Na_2O, and 0–0.8% K_2O.

Chromite, ilmenite, and troilite are disseminated in particle matrices. In the case of particle NZ6-2-5,15, chromite platelets show subparallel orientation. Small grain sizes prevented accurate determination of their compositions.

Bulk compositions of the particles, as determined by the broad beam microprobe technique, are presented in Table 3. The particle NZ6-2-4,33 and, especially, particle NZ6-2-5,15 are dominated by large pyroxene fragments and, hence, their bulk chemistry as determined from one cut surface is likely to be nonrepresentative. The compositions are characterized by low TiO_2 and Na_2O abundances that are below 0.3 wt% and 0.6 wt%, respectively, and by Mg/(Mg + Fe) ratios that range from 0.4 to 0.7.

DISCUSSION

Origin and Source(s) of the Particles

The particles are classified as basaltic melt breccia because all of them consist of mineral fragments embedded in a melt matrix. According to optical observations and Raman spectra, particles NZ6-2-4,33, NZ6-2-5,15, and NZ6-2-4,5 contain plagioclase in an amorphous state and particle 2–4,33 contains amorphous silica. Because of their poor quality, the Raman spectra of the glassy phases are inconclusive to ascertain whether the phases are diaplectic glass or fused glass. However, angular shapes of the grains, their sharp boundaries with a matrix, and the good stoichoimetry suggest that the glassy phases are diaplectic glass that is formed by a shock compression (Stöffler 1972). Hence, one can assert that these rocks are breccias formed by impact events. Plagioclase fragments in particle NZ6-1-1,44 are not transformed to diaplectic glass and there are no direct proofs of an impact origin of this rock, as in the case of other

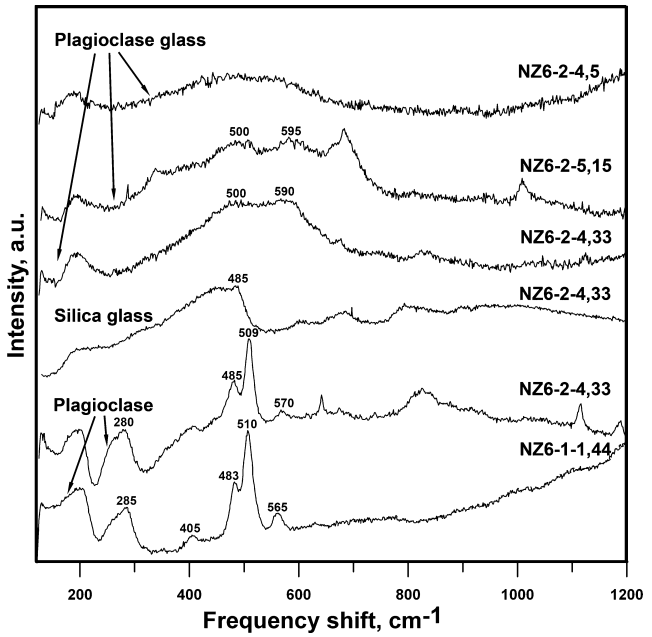

Fig. 3. Raman spectra of plagioclase and silica phases in the studied basaltic melt breccia particles. The spectrum of a plagioclase grain in particle NZ6-1-1,44 displays sufficiently narrow bands. The spectrum of a plagioclase grain marked as (1) on Fig. 2 in particle NZ6-2-4,33 displays characteristic bands too, whereas the spectra of another plagioclase grain marked as (2) on Fig. 2 and a silica grain has broad bands that are typical for amorphous phases. The spectra of plagioclase phases in particles NZ6-2-5,15 and NZ6-2-4,5 are characterized by broad bands over the 300–700 cm^{-1} range. Bands at 680 and 1015 cm^{-1} on the spectrum of particle NZ6-2-5,15 appear to belong to pyroxene.

particles. The particle is a basaltic melt-matrix microbreccia. In principle, nonimpact formation of this rock type on Earth is possible (1) by impregnation of a melt into a fine powder during volcanic eruptions or (2) in shear zones by rapid tectonic movements, where melting temperature can be achieved. However, the authors do not know examples of such basaltic microbreccias of nonimpact origin. In any case, even if these rocks exist, they should be very rare. On the other hand, melt breccia is a typical rock in impact craters, and we suppose that particle NZ6-1-1,44 is an impact melt rock, too.

As follows from the above, three particles have an impact origin and one particle is proposed as an impact melt rock. However, the only found terrestrial impact structure formed in a basaltic target is the 1.8 km diameter Lonar Crater in India (Osae et al. 2005).

There are also other features that distinguish the particles from terrestrial basalts: (1) there are no traces of terrestrial alteration; (2) bytownite ($An_{85–91}$), the dominant plagioclase, and troilite are rare in terrestrial basalts, (3) low K_2O contents (< 0.1 wt%) in the three

Table 3. Glass and bulk compositions (wt%) in the Novaya Zemlya basaltic UMMs.

	NZ 6-1-1,44		NZ 6-2-4,33	NZ 6-2-5,15	NZ 6-2-4,5	
UMM	Glass	Bulk[a]	Bulk[a]	Bulk[a]	Glass	Bulk[a]
SiO_2	51.4	49.4	52.6	50.7	68.5	54.0
TiO_2	0.60	0.40	0.16	0.35	0.53	0.39
Al_2O_3	13.0	13.7	6.43	2.35	22.2	17.1
Cr2O3	0.04	0.23	0.41	0.46	0.02	0.89
FeO	15.9	17.4	16.2	26.8	0.30	5.69
MnO	0.67	0.70	0.52	0.87	n.d.	0.10
MgO	6.50	6.99	18.3	9.79	0.04	6.03
CaO	10.8	10.6	5.19	8.55	2.18	9.86
Na_2O	0.30	0.45	0.15	0.10	5.32	4.06
K_2O	0.03	0.04	0.02	0.02	0.19	1.44
Total	99.21				99.33	

[a]Recalculated to 100 wt%. n.d. = not detected.

basaltic particles are also nontypical for terrestrial basalts. Further, basalts are not present in Northern Island of the Novaya Zemlya archipelago. The Franz Josef Land archipelago is located in 400 km from Northern Island and is the nearest area comprising basalts. However, the Franz Josef Land basalts contain more Na_2O, K_2O, and TiO_2 (Ntaflos and Richter 2003) and are chemically clearly distinct from the described basalts.

Particles NZ6-2-5,15 and NZ6-2-4,5 have discontinuous iron oxide rim that is a characteristic feature for MMs (Genge et al. 2008). Based on this and taking into account the presence of diaplectic glasses in particle NZ6-2-4,33 we suggest that the particles are UMMs and that particle NZ6-1-1,44 very likely has an extraterrestrial origin.

The basaltic UMMs have different mineral compositions. Particle NZ6-2-4,5 has the lowest Ca content in its plagioclase ($An_{70–75}$) and the lowest Fe content in pyroxenes ($Fs_{13–17}Wo_{5–7}$ and $Fs_{5–6}Wo_{38–44}$) of all particles investigated. Particle NZ6-1-1,44 is at an intermediate level in plagioclase ($An_{77–85}$) and pyroxene ($Fs_{21–35}Wo_{1–3}$) compositions, whereas the two remaining particles have a more Ca-rich plagioclase ($An_{89–91}$) and ferrous pyroxenes ($Fs_{49–60}Wo_{2–6}$ and $Fs_{42–48}Wo_{18–24}$). Fe/Mn ratios in pyroxenes vary significantly from 12–15 to 30–35 and these ratios are specific for pyroxenes in any single UMM. Clustering of the Fe/Mn ratios for each individual UMM is shown in Fig. 4. Such variations in pyroxene and plagioclase compositions and the distinct textures indicate that the studied UMMs have different parents.

The main minerals in all particles are low- and high-Ca pyroxenes and high-Ca plagioclase. This suggests that the parent bodies of the particles were basaltic in general. Bulk chemical compositions of three UMMs are rather similar to compositions of primitive

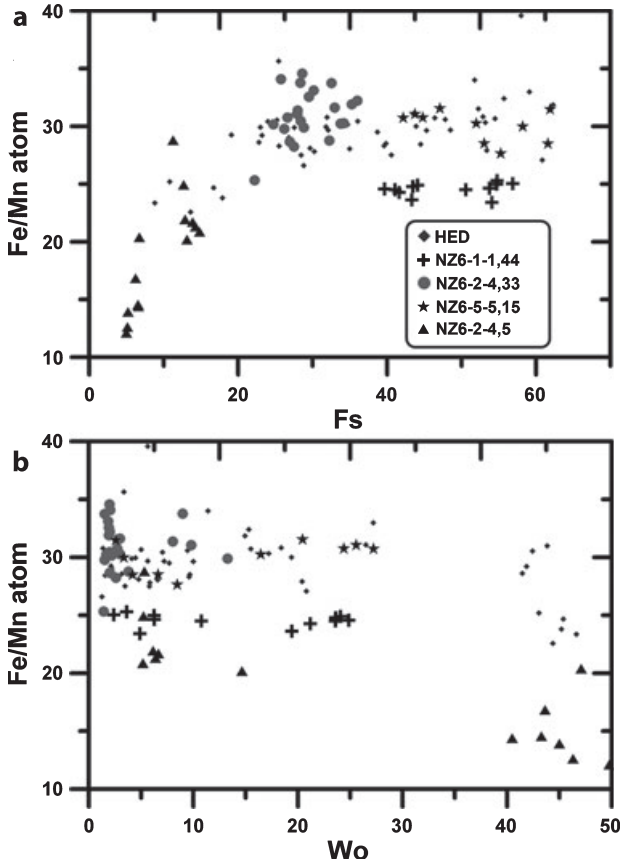

Fig. 4. The Fe/Mn variations versus ferrosilite and wollastonite contents in pyroxenes from the studied basaltic UMMs compared with pyroxenes from HED meteorites (Pun and Papike 1996; Mittlefehldt et al. 1998). Points for basaltic UMM pyroxenes are single electron microprobe analyses.

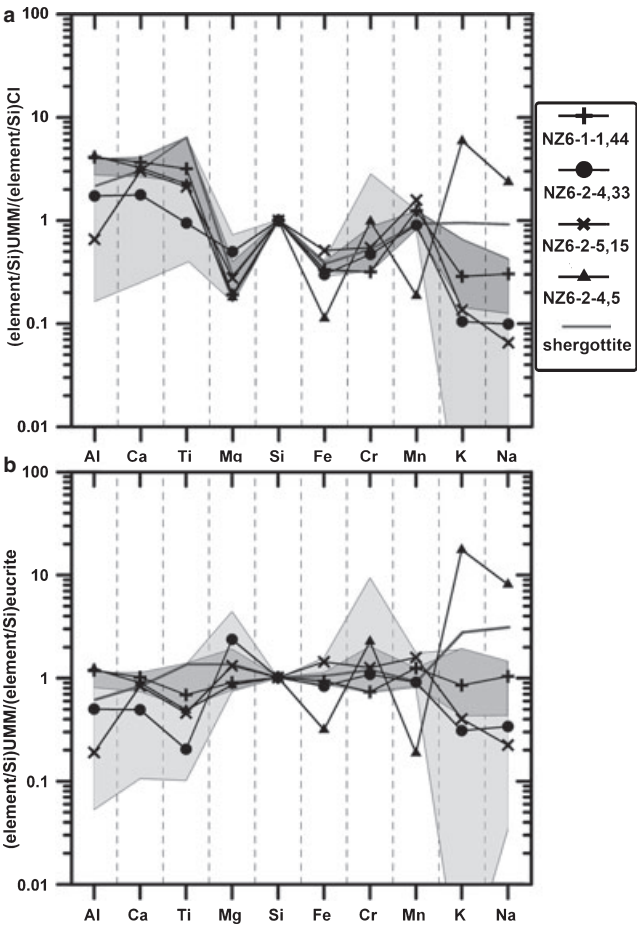

Fig. 5. Bulk compositions of the Novaya Zemlya basaltic UMMs (Table 3) normalized to Si and CI (a) and to an average eucrite (b). The gray areas denote element abundance ranges in eucrites (minimal and maximal values) and the light gray areas denote the same in HED meteorites. The chemical composition of CI is adopted from Anders and Grevesse (1989) and the average eucrite and shergottite compositions are from Mittlefehldt et al. (1998), Kitts and Lodders (1998), and Meyer (2009).

basaltic rocks such as eucrites and shergottites and the bulk composition of NZ6-2-4,5 is close to basaltic andesite, which, however, is likely not representative because of its small size (Table 3). Major and minor element abundance patterns normalized to Si match in general those of eucrites and shergottites, especially for particle NZ6-1-1,44 (Figs. 5a and 5b). In comparison with meteoritic basalts, particle NZ6-2-5,15 is enriched in Fe and Mn and depleted in Al and alkalis, which is probably due to the fact that it is very pyroxene-rich. Particles NZ6-2-4,33 and NZ6-2-4,5 show the largest deviations from meteoritic basalt compositions. Particle NZ6-2-4,33 has slightly higher contents of Si and Mg and lower contents of Ca and Na as compared with others. A noteworthy feature of the NZ6-2-4,5 bulk composition is the relative elevated contents of Si, Na, and K with a Na/K wt% ratio of 2.5 as well as low contents of Fe and Mn.

Petrographically, the particles are melt breccias with a glassy matrix. Pyroxenes in particles NZ6-1-1,44 and NZ6-2-5,15 have exsolution lamellae that suggest relatively slow cooling of the parent basalts. The presence of glass and mineral dust in the glassy matrix implies relatively fast quenching of the breccia(s). The presence of reaction borders and traces of partial melting in a pyroxene grain could be considered as a result of a high temperature when the matrix was liquid. Glass in particle NZ6-1-1,44 does not contain any newly-formed phases and it is compositionally close to the bulk composition of the particle (Table 3). Matrix glass of particle NZ6-2-4,5, if compared to particle bulk composition, is richer in Si and alkalis and poorer in Mg and Fe. Broad beam microprobe analyses demonstrate that regions consisting of glass and newly formed tiny crystals (pyroxene?) are compositionally

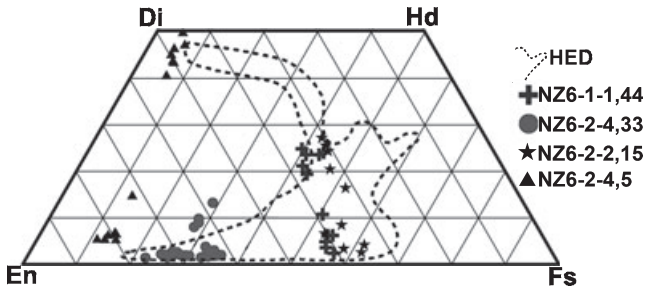

Fig. 6. Compositions of pyroxenes of the basaltic UMMs from Novaya Zemlya. The composition fields of eucrite basalt pyroxenes (Papike 1981; Mittlefehldt et al. 1998) are outlined by a dashed line. Points for basaltic UMM pyroxenes are single electron microprobe analyses.

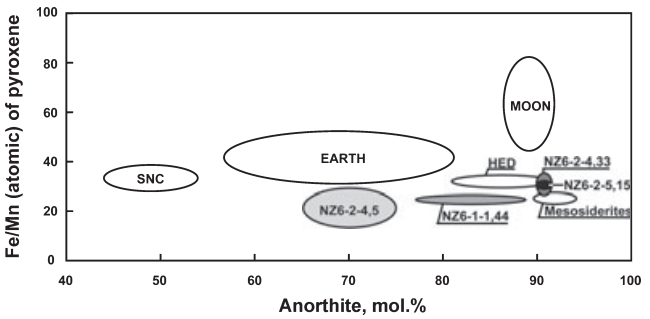

Fig. 7. The Fe/Mn ratios of pyroxene versus An contents of plagioclase from the basaltic UMMs compared to planetary and meteoritic basalts (modified from Papike et al. 2003); ranges in compositions represent one standard deviation from the mean. Heights and widths of the basaltic UMM marks correspond to the full range of the variability.

close to the bulk particle composition. We suggest that the matrix was partially crystallized with precipitation of pyroxene (?) that implies slow cooling of the breccia NZ6-2-4,5 or a short term thermal metamorphism.

Glass matrix breccias could have formed by total or partial melting of precursor basalts accompanied by mixing of the melts with rock and mineral fragments in a high-energy process (e.g., a shock event). This view is supported by the chemical similarity of glasses and bulk rock compositions for three UMMs. The presence of diaplectic plagioclase and quartz glasses, dusty mineral fragments in NZ6-2-4,33, and NZ6-2-4,5, and incipient melting of pyroxene in NZ6-2-5,15 can be considered as evidence of their formation in impact events. Such a process could have formed the microbreccias by collisions in space. Particle NZ6-1-1,44 probably has the same origin. However, an alternative possible process could be the explosion of a solid achondritic meteoroid in the Earth's atmosphere due to triboelectric discharges (ruptures) as recently proposed by Spurný and Ceplecha (2008).

Previous Discoveries of Basaltic MMs and Comparison with Basaltic Meteorites

Cosmic spherules of basaltic compositions were reported from the South Pole Water Well (SPWW) MM collection (Taylor et al. 2007a). They consist of glass with occasional inclusions of silica and plagioclase. Based on the glass composition and the Fe/Mn and Fe/Mg ratios, it has been suggested that a howardite, eucrite, and diogenite (HED) meteorite parent body is the most likely precursor of these spheres. One basaltic UMM particle from the MM collection from Cap Prudhomme, Antarctica (Gounelle et al. 2009) consists of pigeonite with augite exsolution lamellae, high-Ca plagioclase, and quartz. It is similar to our particles in its texture and mineralogy. Gounelle et al. (2009) asserted that its mineral chemistry and oxygen isotopic composition do not correspond to any known extraterrestrial basaltic rock and suggest that it could be from a parent body that has no sample in our meteorite collections yet.

The HED meteorites are the most widespread among achondritic meteorites and, hence, it is of some interest of how the basaltic UMMs relate to HED meteorites. Low-Ca pyroxenes of UMMs NZ6-2-4,33, NZ6-2-5,15, and NZ6-1-1,44 and high-Ca pyroxenes of UMM NZ6-2-5,15 have compositions that are similar to those of eucritic pyroxenes. High-Ca pyroxenes from the UMMs NZ6-2-4,33 and NZ6-1-1,44 do not project exactly into the eucrite pyroxene field. Low- and high-Ca pyroxene compositions of the UMM NZ6-2-4,5 (Fig. 6) project far out of the field defined by eucritic pyroxene compositions but overlap with those of diogenitic pyroxenes.

The Fe/Mn ratios in magmatic pyroxenes have been shown to be diagnostic in distinguishing rocks from different planets and parent bodies, such as the Moon, the Earth, the SNC meteorites parent (Mars?), and the HED meteorite parent (4 Vesta?), which have specific atomic Fe/Mn ratios of 62 ± 18 (1 SD), 40 ± 11, 32 ± 6, and 30 ± 2, respectively (Papike et al. 2003).

The pyroxene Fe/Mn atomic ratios for the UMMs NZ6-2-4,33 and NZ6-2-5,15 are 31 ± 2.2 (1 SD) and 30 ± 1.3, respectively, close to the eucrite values. Pyroxenes of UMMs NZ6-1-1,44 and NZ6-2-4,5 have lower Fe/Mn ratios of 24.6 ± 0.5 and 18.7 ± 4.9 (1 SD), respectively. Plagioclase from UMM NZ6-2-4,5 is compositionally more sodic than eucritic plagioclase, whereas the plagioclase compositions from the three other UMMs are close to those of eucritic plagioclase.

If we combine the Fe/Mn ratios with plagioclase compositions in basalts (Papike et al. 2003) we find that

the studied basaltic UMMs occupy individual locations (Fig. 7). The UMMs NZ6-2-5,15 and NZ6-2-4,33 are located close to the HED and mesosiderite fields, NZ6-1-1,44 projects slightly off the HED field and NZ6-2-4,5 far away from these meteorite groups. Antarctic basaltic UMM MM40 with Fe/Mn = 26.5 ± 0.6 (Gounelle et al. 2009) could be related to particle NZ6-1-1,44 (Fe/Mn = 24.6 ± 0.5). We suppose that UMM NZ6-2-5,15 and NZ6-2-4,33 may have a common parent body. Taking into account the proximity of the UMM fields to the HED and mesosiderite fields, the studied UMMs could be relatives of either one. UMMs NZ6-1-1,44 and NZ6-2-4,5 seem to be related to extraterrestrial rocks, which appear not to be represented in our meteorite collections. Mineralogy and chemistry of UMM NZ6-2-4,5 are distinct from recently described andesite-like meteorites GRA 06128/9 (Day et al. 2009) and alkali-rich impact glasses from howardites (Barrat et al. 2009). Oxygen isotopic studies might shed light on possible relationships of the basaltic UMMs with known celestial rocks.

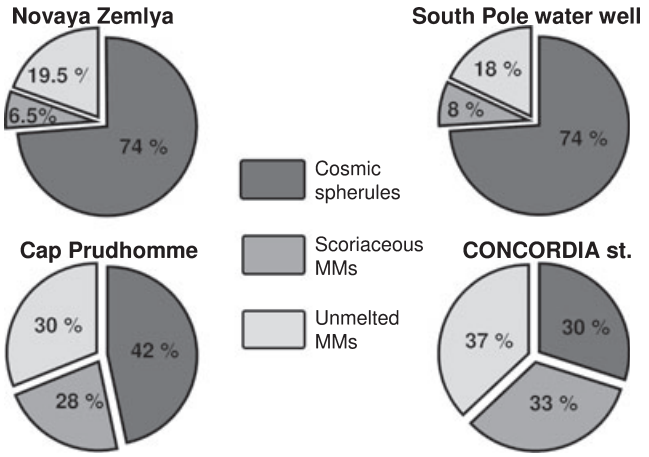

Fig. 8. Percentage of MM groups in the Novaya Zemlya MM collection in comparison with Antarctic MM collections. Data for Antarctic collections were taken from Taylor et al. (2007b)—the South Pole station water well; Maurette et al. (1991), Kurat et al. (1994), Maurette et al. (1996), and Engrand and Maurette (1998)—Cap Prudhomme; Dobrica et al. (2008)—the CONCORDIA station.

Flux of Basaltic UMMs

The studied 50–400 μm suite of micrometeorites has 176 (19.6%) UMMs, 59 (6.6%) scoriaceous MMs, and 660 (73.7%) cosmic spherules. Basaltic UMMs constitute 0.45% of all dust objects (MMs and CSs) and 2.3% of the UMMs. It should be noted, however, that these proportions very likely do not correspond to actual ones because our collection can be biased due to different reasons—e.g., depletion of some MM group(s) during their deposition and concentration on the glacier surface, redeposition of MM-containing sediments, etc. It seems that the most common carbonaceous chondrite-like UMMs are mechanically unstable and can be lost easier that other MM types. For this reason, we compare the populations of main MM groups in the Novaya Zemlya collection and three less biased collections of Antarctic MMs (Fig. 8). The MM group percentages are very close in the SPWW and Novaya Zemlya collections. The Cap Prudhomme and CONCORDIA collections are richer in scoriaceous MMs and UMMs (Fig. 8). We do not discuss the problem of the discrepancy but it has been suggested (Duprat et al. 2007) that the CONCORDIA Antarctic collections are almost unbiased and statistically representative. This allows the estimation of the content of basaltic UMMs in the Novaya Zemlya collection actually to lie in a range of 0.5–0.2%. The smaller value was obtained under the assumption that the primary cosmic spherule content in this collection was 30% or the same as the CS contents in the Cap Prudhomme and CONCORDIA collections.

This calculated percentage proportion agrees well with the estimate for the content of HED-like CSs content in the SPWW micrometeorite collection (Taylor et al. 2007a). On the other hand, only one basaltic UMM has been found among Antarctic micrometeorites. Their number should be much higher if compared to what we have found. If all basaltic MMs at Novaya Zemlya have similar textures and mineral compositions, it could be assumed that they were formed by a disruption of one basaltic meteoroid in the Earth's atmosphere, e.g., according to the mechanism proposed by Spurný and Ceplecha (2008). However, as we have shown, the UMMs should have different parent bodies and the single parent scenario can be rejected. We do not have a valid explanation for the fact that Antarctic MMs contain such low numbers of basaltic UMMs but speculate that the observed enrichment of the basaltic UMM type in the NZ sample with respect to Antarctic MMs could be connected either to the process of removal of specifically light carbonaceous MMs during deposition on the NZ glacier or to a spatial or temporal fluctuation in the global MM flux.

CONCLUSIONS

Four basaltic breccia UMMs were identified from a suite of micrometeorites collected from the Novaya Zemlya glacier. Textures and compositions of these melt breccia UMMs demonstrate the possibility that they originated from the surface layers of basaltic asteroids that have been reworked by high-velocity impacts. On the other hand, the breccias could have been formed by

triboelectric decomposition of achondritic meteoroids in the Earth's atmosphere (Spurný and Ceplecha 2008).

Based on pyroxene and plagioclase compositions as well as on Fe/Mn ratios in pyroxenes, we suggest that the studied UMMs originated from three compositionally distinct parents. Two of the UMMs may have a common parent that is eucritic or mesosideritic.

A comparison of abundances of MM groups (unmelted, scoria, and melted) with Antarctic collections shows that abundances of the MM groups in the Novaya Zemlya collection are close to those found in the SPWW collection, but is poorer in UMMs compared to other Antarctic collections. This apparently is due to a depletion of fragile or unstable carbonaceous UMMs (Gounelle et al. 2005). Having taken this into consideration, we estimate that the basaltic UMM flux lies in the range of 0.5–0.2% of the total MM flux. If the ordinary chondrite to achondrite ratio in the MM stream is similar to the ratio in the meteorite stream (OC/HEDs approximately 45), then the number of ordinary chondrite MMs should be 22.5–9%—very far from the observed value of $< 1\%$ (Walter et al. 1995). A real conundrum is left to be solved.

Acknowledgments—This work was supported by the Academy of Sciences of Austria and Academy of Finland, FWF in Austria, RFFI (grant 09-05-00444-a) and RAS Programme N5 in Russia. We thank the reviewers, M. J. Genge and T. Nakamura, and the associate editor, D. E. Brownlee, for their constructive comments that helped to improve the manuscript. D. D. B. thanks the Northern department of hydrological and meteorological service (Arkhangelsk, Russia) and its chief Dr. L. Yu. Vasil'ev, as well as Yu. N. Nasteko, captain of the "Mikhail Somov" vessel, for their support and help during the 2006 expedition.

Editorial Handling—Dr. Donald Brownlee

REFERENCES

Anders E. and Grevesse N. 1989. Abundances of the elements: Meteoritical and solar. *Geochimica et Cosmochimica Acta* 53:197–214.

Badjukov D. D. and Raitala J. 2003. Micrometeorites from the northern ice cap of the Novaya Zemlya archipelago, Russia: The first occurrence. *Meteoritics & Planetary Science* 38:329–340.

Barrat J. A., Yamaguchi A., Greenwood R. C., Bollinger C., Bohn M., and Franchi I. A. 2009. Trace element geochemistry of K-rich impact spherules from howardites. *Geochimica et Cosmochimica Acta* 73:5944–5958.

Blanchard M. B., Brownlee D. E., Bunch T. E., Hodge P. W., and Kyte F. T. 1980. Meteoroid ablation spheres from deep-sea sediments. *Earth and Planetary Science Letters* 46:178–190.

Brownlee D. E., Bates B., and Schramm L. 1997. The elemental composition of stony cosmic spherules. *Meteoritics & Planetary Science* 32:157–175.

Day J. M. D., Ash R. D., Liu Y., Bellucci J. J., Rumble D. III., McDonough W. F., Walker R. J., and Taylor L. A. 2009. Early formation of evolved asteroidal crust. *Nature* 457:179–182.

Dobrica E., Engrand C., Leroux H., Duprat J., and Gounelle M. 2008. Classic and exotic particles in the 2006 CONCORDIA Antarctic micrometeorite collection (abstract #1672). 39th Lunar and Planetary Science Conference. CD-ROM.

Duprat J., Engrand C., Maurette M., Kurat G., Gounelle M., and Hammer C. 2007. Micrometeorites from Central Antarctic snow: The CONCORDIA collection. *Advances in Space Research* 39:605–611.

Engrand C. and Maurette M. 1998. Carbonaceous micrometeorites from Antarctica. *Meteoritics & Planetary Science* 33:565–580.

Fritz J., Greshake A., and Stöffler D. 2005. Micro-Raman spectroscopy of plagioclase and maskelynite in Martian meteorites: Evidence of progressive shock metamorphism. *Antarctic Meteorite Research* 18:96–116.

Genge M. J. 2008. Koronis asteroid dust within Antarctic ice. *Geology* 36:687–690.

Genge M. J., Gileski A., and Grady M. M. 2005. Chondrules in Antarctic micrometeorites. *Meteoritics & Planetary Science* 40:225–238.

Genge M. J., Engrand C., Gounelle M., and Taylor S. 2008. The classification of micrometeorites. *Meteoritics & Planetary Science* 43:497–515.

Gounelle M., Engrand C., Maurette M., Kurat G., McKeegan K. D., and Brandstaetter F. 2005. Small Antarctic micrometeorites: A mineralogical and in situ oxygen isotope study. *Meteoritics & Planetary Science* 40:917–932.

Gounelle M., Chaussidon M., Morbidelli A., Barrat J.-A., Engrand C., Zolensky M. E., and McKeegan K. D. 2009. A unique basaltic micrometeorite expands the inventory of solar system planetary crusts. *Proceedings of the National Academy of Sciences* 106:6904–6909.

Grady M. M. 2000. *Catalogue of meteorites*, 5th ed. Cambridge, UK: University Press. 689 p.

Gucsik A., Koeberl C., Brandstätter F., Libowitzky E., and Reimold W. U. 2003. Scanning electron microscopy, cathodoluminescence, and Raman spectroscopy of experimentally shock-metamorphosed quartzite. *Meteoritics & Planetary Science* 38:1187–1197.

Halliday I., Blackwell A. T., and Griffin A. A. 1989. The flux of meteorites on the Earth's surface. *Meteoritics* 24:173–178.

Kitts K. and Lodders K. 1998. Survey and evaluation of eucrite bulk composition (abstract). *Meteoritics & Planetary Science* 33:A197.

Koryakin V. S. 1990. *Arctic glaciers*. Moscow: Nauka Press. 158 p. (in Russian)

Kurat G., Koeberl C., Presper T., Brandstätter F., and Maurette M. 1994. Petrology and geochemistry of Antarctic micrometeorites. *Geochimica et Cosmochimica Acta* 58:3879–3904.

Kurat G., Hoppe P., and Engrand C. 1996. A chondrule micrometeorite from Antarctica with vapor-fractionated trace-element abundances (abstract). *Meteoritics & Planetary Science* 31:A75.

Love S. G. and Brownlee D. E. 1991. Heating and thermal transformation of micrometeoroids entering the Earth's atmosphere. *Icarus* 89:26–43.

Love S. G. and Brownlee D. E. 1993. A direct measurement of the terrestrial mass accretion rate of cosmic dust. *Science* 262:550–553.

Matson D. W., Sharma S. H., and Philipotts J. A. 1986. Raman spectra of some tectosilicates and of glasses along the orthoclase-anorthite and nepheline-anorthite joins. *American Mineralogist* 71:694–704.

Maurette M. 2006. *Micrometeorites and the mysteries of our origins*. Berlin Heidelberg: Springer-Verlag. 298 p.

Maurette M., Hammer C., Reeh N., Brownlee D. E., and Thomsen H. H. 1986. Placers of cosmic dust in the blue ice lakes of Greenland. *Science* 233:869–872.

Maurette M., Jehanno C., Robin E., and Hammer C. 1987. Characteristics and mass distribution of extraterrestrial dust from the Greenland ice cap. *Nature* 328:699–702.

Maurette M., Olinger C., Michel-Levy M. C., Kurat G., Pourchet M., Brandstätter F., and Bourot-Denise M. 1991. A collection of diverse micrometeorites recovered from 100 tonnes of Antarctic blue ice. *Nature* 351:44–47.

Maurette M., Engrand C., and Kurat G. 1996. Collection and microanalysis of Antarctic micrometeorites. Proceedings, the 150th colloquium of the International Astronomical Union. pp. 265–273.

Meyer C. 2010. *Mars Meteorite Compendium*. http://curator.jsc.nasa.gov/antmet/mmc/index.cfm

Mittlefehldt D. W., McCoy T. J., Goodrich C. A., and Kracher 1998. Non-chondritic meteorites from asteroidal bodies. In *Planetary materials*, edited by Papike J. J. Washington, D.C.: Mineralogical Society of America. pp. 1–170.

Ntaflos T. and Richter W. 2003. Geochemical constraints on the origin of the Continental Flood Basalt magmatism in Franz Josef Land, Arctic Russia. *European Journal of Mineralogy* 15:649–663.

Osae S., Misra S., Koeberl C., Sengupta D., and Ghosh S. 2005. Target rocks, impact glasses, and melt rocks from the Lonar impact crater, India: Petrography and geochemistry. *Meteoritics & Planetary Science* 40:1473–1492.

Papike J. J. 1981. Silicate mineralogy of planetary basalts. In *Basaltic volcanism on the terrestrial planets*, edited by Merrill R. B. and Ridings R. New York: Pergamon Press. pp. 340–363.

Papike J. J., Karner J. M., and Shearer C. K. 2003. Determination of planetary basalt parentage: A simple technique using the electron microprobe. *American Mineralogist* 88:469–472.

Peucker-Ehrenbrink B. and Ravizza G. 2000. The effects of sampling artifacts on cosmic dust flux estimates: A reevaluation of nonvolatile tracers (Os, Ir). *Geochimica et Cosmochimica Acta* 64:1965–1970.

Pun A. and Papike J. J. 1996. Unequilibrated eucrites and the equilibrated Juvinas eucrite: Pyroxene REE systematics and major, minor, and trace element zoning. *American Mineralogist* 81:1438–1451.

Spurný P. and Ceplecha Z. 2008. Is electric charge separation the main process for kinetic energy transformation into the meteor phenomenon? *Astronomy & Astrophysics* 489:449–454.

Stöffler D. 1972. Deformation and transformation of rock-forming minerals by natural and experimental shock processes. *Fortschritte der Mineralogie* 49:50–113.

Suavet C., Alexandre A., Franchi I. A., Gattacceca J., Sonzogni C., Greenwood R. C., Folco L., and Rochette P. 2010. Identification of the parent bodies of micrometeorites with high-precision oxygen isotope ratios. *Earth and Planetary Science Letters* 293:313–320.

Taylor S. and Brownlee D. E. 1991. Cosmic spherules in the geologic record. *Meteoritics* 26:203–211.

Taylor S., Lever J. H., and Harvey R. P. 1998. Accretion rate of cosmic spherules measured at the South Pole. *Nature* 392:899–903.

Taylor S., Lever J. H., and Harvey R. P. 2000. Numbers, types, and compositions of an unbiased collection of cosmic spherules. *Meteoritics & Planetary Science* 35:651–666.

Taylor S., Herzog G. F., and Delaney J. S. 2007a. Crumbs from the crust of Vesta: Achondritic cosmic spherules from the South Pole water well. *Meteoritics & Planetary Science* 42:223–233.

Taylor S., Matrajt G., Lever J. H., Brownlee D. E., and Joswiak D. 2007b. Types of micrometeorites accreting at the South Pole, Antarctica (abstract #1338). 38th Lunar and Planetary Science Conference. CD-ROM.

Velde B., Syono Y., Kikuchi M., and Boyer H. 1989. Raman microprobe study of synthetic diaplectic plagioclase feldspars. *Physics and Chemistry of Minerals* 16:436–441.

Walter J., Kurat G., Brandstätter F., Koeberl C., and Maurette M. 1995. The abundance of ordinary chondrite debris among Antarctic micrometeorites (abstract). *Meteoritics* 30:592–593.

Yada T., Nakamura T., Takaoka N., Noguchi T., Terada K., Yano H., Nakazawa T., and Kojima H. 2004. The global accretion rate of extraterrestrial materials in the last glacial period estimated from the abundance of micrometeorites in Antarctic glacier ice. *Earth, Planets and Space* 56:67–79.